



PII S0016-7037(02)00988-2

Effects of different crystal faces on the surface charge of colloidal goethite (α -FeOOH) particles: An experimental and modeling study

FABIEN GABORIAUD* and JEAN-JACQUES EHRHARDT

Laboratoire de Chimie Physique et Microbiologie pour l'Environnement, UMR 7564, CNRS, Université Henri Poincaré, Nancy 1, 405 rue de Vandoeuvre, F-54600 Villers-lès-Nancy, France

(Received November 26, 2001; accepted in revised form May 30, 2002)

Abstract—The surface charge of colloidal particles is usually determined by potentiometric titration. These acid-base titrations make it possible to measure the pH of point-of-zero charge (pzc) for oxide minerals. This macroscopic property is the most important parameter used in surface complexation modeling to reproduce experimental data. The pzc values of goethite reported in the literature vary between 7.0 and 9.5. Carbonate adsorption and/or surface morphology are thought to account for this wide range.

We demonstrate a procedure for the removal of the carbonate ions that initially adsorb on goethite and strongly affect the titration curves and pzc determination. We also investigated the crystal-face-specific reactivity of two morphologically different goethites. The z-profiles obtained from atomic force microscopy (AFM) images showed that the goethite with the smallest specific surface area ($S = 49 \text{ m}^2/\text{g}$, denoted G49) exhibits 70% of the (001) face, whereas this value is only 30% for the goethite with largest specific surface area ($S = 95 \text{ m}^2/\text{g}$, denoted G95). This morphologic difference results in slightly different pzc values: 9.0 for G49 goethite and 9.1 for G95 goethite. These experimental pzc values have been correlated with multisite complexation calculations using both the full-site and the 1-pK approaches. We used the full-site approach to consider all of the configurations of hydrogen bond interactions with surface site. The resulting mean charges gave estimated pzc values of 8.9 and 9.2 for the (001) and (101) faces, respectively. Considering these theoretical pzc values for individual faces and the face distributions obtained from AFM analysis, the calculated pzc values are in full agreement with the experimental pzc values. However, this morphologic difference is more expressed in surface charge values than in the pzc values. Indeed, the surface charge of G49 goethite is much higher than that of G95 goethite, and the 1-pK calculations make it possible to fit the titration data satisfactorily. Copyright © 2003 Elsevier Science Ltd

1. INTRODUCTION

Most of the chemical and physical processes that occur in the environment are governed by mineral-water interfaces. In the case of inorganic oxide colloids, many processes, such as ion sorption (Dzombak and Morel, 1990), particle-particle interactions (Hiemenz, 1977), and mineral dissolution (Stumm, 1992), result from the distribution and heterogeneity of protonated and unprotonated surface sites. The surface charge of colloid particles, which is due to the protonation and/or deprotonation of some surface sites, is mainly a function of the pH and ionic strength of the aqueous solution (Hochella and White, 1990; Israelachvili, 1992). The speciation of such surface sites, i.e., their structure and concentration, has been the subject of numerous experimental and theoretical studies for the past 30 year (Sparks and Grundl, 1999). However, several points are still unclear, e.g., the specific surface charges of the crystalline faces of particles and the nature of surface sites. Most groups consider oxide minerals to be homogeneous particles; therefore, the inherent structural heterogeneity of minerals, such as different crystalline faces including surface defects or different surface groups, is not taken into account (Sposito, 1984).

A variety of surface complexation models have been used to replicate, understand, and predict the acid-base properties and metal-binding behavior of oxide colloids (Dzombak and Morel,

1990; Sverjensky and Sahai, 1996; Venema et al., 1996a). Most of these models concern interface reactions involving fixed surface sites that develop electrostatic fields adjacent to a particle with different planes. The structure and distribution of the ions in the interfacial region differ from model to model, as does the representation of surface sites.

In the 2-pK model, amphoteric single surface sites with integer formal charges (three protonation states) are distributed randomly on the surface (Yates et al., 1974; Davis and Leckie, 1978a, 1978b; Dzombak and Morel, 1990; Hayes et al., 1991; Robertson and Leckie, 1997). The proton affinity constants of the two protonation equilibrium reactions are determined from the experimental surface charge vs. pH from either potentiometric titrations or electrophoretic mobility. The most widely used 2-pK model includes different types of electrostatic layers, such as double layers (Dzombak and Morel, 1990; Stumm, 1992), triple layers (Yates et al., 1974; Hayes and Leckie, 1987; Hayes et al., 1988), and quadruple layers (Charmas, 1999; Rudzinski et al., 1999). These approaches are increasingly complicated by the fact that the surface complexation parameters range from three to seven. To reduce the number of free parameters, Sverjensky and Sahai (1996) predicted the two proton affinity constants from a theoretical equation, which considered an electrostatic theory, a Born solvation argument, and an average bulk solid dielectric constant. However, all of these calculations or predictions assume that the surface is chemically homogeneous and that the charging occurs via a

* Author to whom correspondence should be addressed (gaboriaud@lcpce.cnrs-nancy.fr).

two-step protonation reaction, regardless of the nature of the mineral oxides.

A crystallography-based approach can be used to assess the composition and structure of the surface. This approach led to the identification of different types of surface groups, namely, singly, doubly, or triply coordinated oxygens from surface sites. The charges of these oxygens are calculated by use of Pauling bond valence theory, which generally gives fractional values for this charge (Pauling, 1929). These considerations led to the establishment of the multisite complexation (MUSIC) model (Hiemstra et al., 1989a, 1989b, 1996), which is based on the formalism of the 1-pK model (Hiemstra et al., 1987; Van Riemsdijk et al., 1987). In this model, the proton affinity constant of each individual surface group is calculated from the undersaturation of the oxygen valence, i.e., the formal charge. Interestingly, a linear relationship was found between the constant values and the actual oxygen charge for both dissolved and surface species (Hiemstra et al., 1996). The actual oxygen charge is calculated from the local contribution of the metallic ligands and from the number of hydrogen bonds with adsorbed water. The MUSIC model has been used to calculate the charging behavior of various metal (hydr)oxides (Nabavi et al., 1993; Contescu et al., 1996; Hiemstra et al., 1996; Venema et al., 1998; Boily et al., 2001; Bourikas et al., 2001). According to this formalism, the specificity of each crystalline face can be used to calculate the theoretical individual contribution of each face on an experimental charging curve. Unfortunately, few studies have tried to correlate the experimental data obtained with particles with different faces and the theoretical MUSIC calculations (Hiemstra and Van Riemsdijk, 1999a). This model has also been extended to account for adsorbed surface complexes using the charge distribution MUSIC approach (Hiemstra and Van Riemsdijk, 1996, 1999b; Rietra et al., 1999b, 2000).

Several experimental studies have quantified the acid-base properties of oxide minerals. The most common method involves the use of potentiometric acid-base titration (Parks and De Bruyn, 1962; Dzombak and Morel, 1990; Stumm, 1992). If protons and hydroxide ions are the only potential-determining ions, the global surface charge can be calculated from the adsorbed protons, i.e., the net consumption of protons and hydroxide by the mineral surface. The common intersection point on experimental titration curves, corresponding to different concentrations of basic electrolyte, is defined as the pH of the point-of-zero net proton charge or, in the case of any other interacting ions, the point-of-zero charge (pzc) if this point corresponds to the zero surface charge without the need for renormalization (Sposito, 1984, 1998). Unfortunately, these macroscopic properties have been widely reported in the literature without taking several considerations into account.

Goethite (α -FeOOH) is the iron mineral that is most often found in soils at ambient temperature because of its high thermodynamic stability. Even though it may be present in only small quantities, goethite leads to the adsorption of ions (anions and/or cations) and can account for the colors of many soils (Sposito, 1984). Because of its important role in environmental processes, its properties have been studied in detail over the past 20 year (Cornell and Schwertmann, 1996). However, it is difficult to use potentiometric titrations to determine the pzc value of synthetic goethites because these samples display a

large variety of shapes and sizes depending on how they were synthesized. In addition, three important types of crystal faces have been reported on synthetic and natural goethites according to space group 62 and *Pnma* setting (Cornell and Schwertmann, 1996): the (101), (001), and (210) faces. It is noteworthy that the space group was recently changed from *Pbnm* to *Pnma* according to the *International Tables of Crystallography* (Hahn, 1996), in which the names of crystal faces were also changed (*Pbnm* to *Pnma*, *a* to *c*, *b* to *a*, and *c* to *b*). In the literature, pzc values vary between 7.0 and 9.5 (Davis and Leckie, 1978a, 1978b; Hsi and Langmuir, 1985; Schwertmann et al., 1985; Hayes and Leckie, 1987; Zeltner and Anderson, 1988; Hiemstra et al., 1989a; Lövgren et al., 1990; Lumsdon and Evans, 1994; Van Geen et al., 1994; Hiemstra et al., 1996; Strauss et al., 1997a, 1997b; Venema et al., 1998; Villalobos and Leckie, 2000), which has led to much confusion about the surface properties of this mineral. This variation demonstrates the difficulty of selecting surface complexation model parameters that can reproduce the charge curves. Some authors have claimed that the specific surface areas of particles set the pzc values of goethite (Zeltner and Anderson, 1988). The lower values might have resulted from the adsorption of carbonate on the goethite surface or from the contamination of the blank or the suspension with carbonate (Evans et al., 1979; Zeltner and Anderson, 1988; Lumsdon and Evans, 1994; Van Geen et al., 1994; Villalobos and Leckie, 2000).

However, no study has systematically investigated the effects of crystalline faces on the acid-base properties of different synthetic goethites. We used atomic force microscopy (AFM) experiments to characterize the ratio between the predominant goethite faces on two type of goethite. Then, we carried out potentiometric titrations on these two goethite suspensions. We also discuss an experimental titration procedure that prevents contamination, which could affect the results and the determination of the macroscopic pzc value. This is the first time that a procedure that corrects the raw data from carbonate contamination initially adsorbed onto goethite particles has been described. Because the titration method provides a weighted average of the protonation-deprotonation behavior resulting from the cooperative effects of the different crystal faces, the individual contributions cannot be determined from these data alone. Thus, we used the surface charge values obtained from potentiometric titrations to assess the morphologic effect.

We also calculated charging behavior for each crystalline faces by use of the MUSIC model with both the full-site and the 1-pK approach. This new calculation, which considers the different number of hydrogen bonds for surface sites, was used to test the effect of crystalline faces on the surface charge curves and the macroscopic pzc values when using the MUSIC model. This experimental and theoretical study demonstrates that crystalline faces affect the reactivity of goethite.

2. EXPERIMENTAL PROCEDURES

2.1. Preparation of Reagents

All reagents used were of analytical grade and stored in plastic bottles. All experiments were carried out in plastic vessels to avoid silica contamination. The solutions and suspensions were prepared using freshly prepared high purity

ion-exchanged water (Milli-Q, 18.3 mΩ resistance). A sodium hydroxide solution was prepared in a nitrogen-purged Jacomex TM controlled-atmosphere glove box by diluting a concentrated free carbonate solution (carbonate-free dilute-it, J. T. Baker).

2.2. Goethite

Colloidal goethite suspensions were prepared by neutralizing 500 mL of a 0.5-mol/L ferric nitrate solution ($\text{Fe}[\text{NO}_3]_3 \cdot 9\text{H}_2\text{O}$) with 400 mL of 2.5-mol/L sodium hydroxide solution. Two different procedures were used, both based on the initial procedure developed by Atkinson et al. (1967). The first one was based on the protocol described by Leckie and coworkers (Van Geen et al., 1994; Villalobos and Leckie, 2000), in which the sodium hydroxide solution is added quickly. The second one was based on the method described by Hiemstra et al. (1989a), in which the sodium hydroxide is added at a fixed rate of 9 mL/min. In both cases, the solution was stirred vigorously during the addition of the sodium hydroxide, which was added in a nitrogen atmosphere in a glove box. The precipitate obtained following the rapid addition of sodium hydroxide was aged in an oven for 24 hours at 60°C, whereas the other precipitate was aged for 72 hours at 60°C. The goethite suspensions were then dialyzed (Spectra/Por membrane 2) against Milli-Q water. The water was changed twice a day until its conductivity was close to 1 μS/m. The suspensions were stored in polypropylene containers at 4°C. We used X-ray powder diffraction and Mössbauer spectroscopy to confirm that all of the precipitates were indeed goethite. Adsorption/desorption $\text{N}_2(\text{g})$ isotherms were used to determine the total specific surface areas according to the Brunauer-Emmett-Teller (BET) adsorption method.

2.3. Potentiometric Titrations

The goethite suspensions (between 10 and 20 g/L) were titrated against four concentrations of background electrolyte (0.01, 0.05, 0.1 and 0.5 mol/L of NaNO_3). All titrations were conducted on 50-mL suspensions of goethite in a Teflon vessel under argon at 25°C. A computer-controlled titrator (736 GP Titrimo, Metrohm) was used to add the acid or base to the reactor. Titrations were performed using a Ross Orion Sure-Flow combination electrode (model 8102) that had been calibrated with three commercial buffers (Titrimo, Merckelab). The reaction was considered to be at the equilibrium when pH drift was <0.5 mV/min, leading to an equilibrium time of <30 min. The concentrations of the solids were accurately determined for each suspension by weighing and calcinating aliquots at 80°C.

2.4. AFM

AFM imaging was performed in ambient conditions with a Thermomicroscope Explorer Ecu⁺ scanning probe microscope using a $1 \times 1 \mu\text{m}$ piezoelectric scanner. The images were collected in noncontact mode with either a scan size of 1 μm and a scan rate of 0.5 μm/s or a scan size of 0.5 μm and a scan rate of 0.2 μm/s. In noncontact mode, the AFM tip oscillated near the surface in the attractive force domain at a constant

amplitude. The reduction of the cantilever oscillation from its set point value was used to determine the topography of the surface. Microfabricated silicon oxide tips (Topometrix) with a resonance frequency of ≈245 kHz were used in this mode. The scanning samples were prepared as described by Weidler et al. (1996, 1998). Clean glass slides (stored in 10-mol/L nitric acid and thoroughly rinsed in double-distilled water) were transferred into 20 mg/L of goethite suspension at pH 4.0. After 1 h, the glass slides were removed, gently rinsed with double-distilled water, and oven dried at 90°C for 2 h.

2.5. The MUSIC Calculation

2.5.1. Full-Site Approach

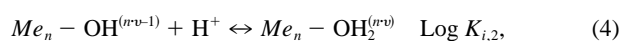
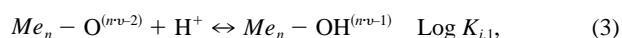
The MUSIC model calculates the proton affinity of a surface group from the formal charge of a surface oxygen, which is given by the sum of its valence and the bond valences of all its ligands (Hiemstra et al., 1996; Venema et al., 1998). In the refined version of this model, the bond valence is related to the bond length and to the donating and/or accepting H bonds exchanged with adsorbed water at the interface. Hiemstra et al. (1996) proposed a simplified equation to calculate the proton affinity constant, K_{H} :

$$\text{Log}K_{\text{H}} = -19.8 \left[-2 + m s_{\text{H}} + n(1 - s_{\text{H}}) + \sum_i^{n_{\text{st}}} s_{i,\text{st}} \right], \quad (1)$$

in which m and n are the number of donating and accepting H bridges with adsorbed water, respectively; s_{H} is the bond valence for a proton bond to a surface oxygen (set to 0.8); n_{st} is the total number of structural bonds; and $s_{i,\text{st}}$ is the bond valence of a structural Fe-O bond as given by the following equation:

$$s_{i,\text{st}} = e^{(R_{0,i-j} - R_{i-j})/0.37}. \quad (2)$$

$R_{0,i-j}$ is an ion-dependent parameter length (set to 1.759 for Fe-O), and R_{i-j} is the Fe-O bond length. The affinity constants are calculated for the two possible protonation reactions of one surface site as follows:



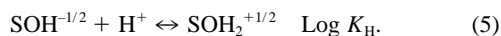
where ν is the bond valence, defined as the charge of the cation divided by its coordination number.

In this approach, the charging curves were constructed according to a simple Stern model with an electrolyte concentration of 0.1 mol/L. To allow comparison with the previous full-site approach of Hiemstra et al. (1996), the Stern capacitance and the ion pair formation constants, considered as symmetrical ion pair formation ($\text{log} K_{\text{C}} = \text{log} K_{\text{A}}$), were set to 1.35 F/m² and -1 , respectively.

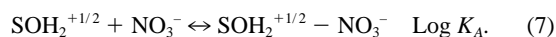
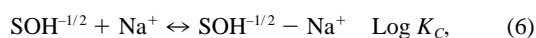
In these surface charge calculations, the different acid-base equilibria of the four crystallographic surface groups of the (101) and (001) faces were considered. In addition, we systematically studied the different values of hydrogen bond interactions, namely, m and n in Eqn. 1.

2.5.2. 1-pK Approximation

This approach considers a single surface site with two protonation states equal to -0.5 and $+0.5$. The distribution is given by the following equilibrium (Hiemstra et al., 1987; Van Riemsdijk et al., 1987):



The proton affinity constant of this equilibrium ($\text{Log } K_{\text{H}}$) was set so that it was equal to the experimental pzc value. As in the full-site approach, the formation of the symmetrical electrolytic ion pair ($\text{Log } K_{\text{C}} = \text{Log } K_{\text{A}}$) in a simple Stern model is considered in the calculations with the following two equilibriums:



Therefore, the search for the best fitting model was based only on the optimization of the Stern capacitance (C_s), the symmetrical electrolyte ion pair ($\text{Log } K_{\text{C}} = \text{Log } K_{\text{A}}$), and the surface site density (N_s). This simplified model for protonation equilibrium has been widely used to decrease the number of adjustable parameters, especially when calculating sorption (Boily et al., 2000, 2001; Hiemstra et al., 1996; Hiemstra and Van Riemsdijk, 1996, 1999b; Rietra et al., 1999a). In addition, the surface site density is generally taken as the crystallographic value, which means that there are only two adjustable parameters: C_s and the ion pair formation constant.

The charging curves were calculated with ECOSAT 4.7 for both approaches (Keizer and Van Riemsdijk, 1994).

3. RESULTS AND DISCUSSION

3.1. Characterization of Goethite

Two types of goethite were synthesized. The specific surface areas, as measured by the BET method, were 49- and 95-m²/g goethites generated by the rapid and low sodium hydroxide addition methods, respectively. These values are in agreement with those obtained by Van Geen et al. (1994) and Hiemstra et al. (1996) using the same methods. The two types of goethite are called G49 and G95 from here on, with reference to their specific surface area values.

A large number of studies have demonstrated that AFM can be used to investigate the three-dimensional morphology of many surfaces (Magonov and Whangbo, 1996; Wiesendanger, 1994). One of the limitations of this technique is that the sample has to be fixed, especially in the case of powders. Thus, only a few groups have characterized goethite particles (Weidler et al., 1996, 1998). On the basis of the work of Weidler et al. (1996, 1998), we used AFM to investigate the morphology of our two synthetic goethites in air.

Figures 1 and 2 show typical deflection AFM images and z-profiles for G49 and G95 goethite particles, respectively. Typical acicular shapes were identified for both types of goethite. In certain experimental conditions, single crystals and aggregates could be seen together. These single crystals measured between 200 and 400 nm in length for G95 and between 500 and 700 nm for G49. These differences were expected given the specific surface area values. These three-dimensional

images allowed us to identify the (101) and the (001) faces on these single goethite crystals. Indeed, the mean experimental angle between these two faces measured from 20 measurements on different crystals was $157^\circ \pm 2^\circ$, which is consistent with the theoretical angle value (155°). As mentioned by Weidler et al. (1998), the experimental angle between (001) and ($\bar{1}01$) is slightly smaller than 10° , but this probably depends on the experimental conditions, e.g., the scan rate and the scanning direction.

The area percentage of the two faces, i.e., (001) and (101), was assessed from the z-profiles by assuming that the total area, measured on one single crystal, is represented by the sum of the areas of the (001), (101), ($\bar{1}01$), ($10\bar{1}$), and ($\bar{1}0\bar{1}$) faces. Furthermore, we assumed that the ($i0i$) faces had the same reactivity and noted these faces as (101). For example, the area percentage of a (001) face on goethite is given by its area divided by the sum of the area face of (001), (101), and ($\bar{1}01$). This calculation, which was repeated at five different locations for a single G49 crystal, led to a (001) surface area percentage of 50% ($\pm 5\%$) for the crystal in Figure 1A and of 70% ($\pm 5\%$) for the crystal in Figure 1B. In the case of G95 goethite, this percentage was close to 30% ($\pm 5\%$) for the crystal in Figure 2A and 50% ($\pm 5\%$) for the one in Figure 2B. In fact, the most frequently observed morphologies were 70% for G49 and 30% for G95. Therefore, the decrease in particle size was accompanied by a decrease in the percentage of (001) faces and an increase in the amount of (101) faces.

These results agree with the crystal growth concept, as the rate of goethite crystallization increased as sodium hydroxide was added more quickly, and thus, the crystals tended to become smaller. Goethite is formed by a dissolution and reprecipitation process, in which ferrihydrite is the first intermediate (Cornell and Schwertmann, 1996). Unfortunately, it is not known whether the reaction rate is governed by the rate of ferrihydrite dissolution, by the nucleation and growth of goethite, or by both processes. Weidler et al. (1998) attempted to answer this question and demonstrated that (001) faces grow more rapidly than (101) faces. Therefore, the decrease in the percentage of (001) faces is associated with lower growth rate, which enhances the slower growing faces, i.e., the (101) face.

3.2. Potentiometric Titrations

3.2.1. Acid-Base Titration Data

Acid-base potentiometric titrations have been widely used to determine the surface charge density (σ) of oxide particles. Because the surface charge is strongly dependent on concentration, these experiments are conducted in the presence of a constant salt concentration at pH 4 to 10. The concentration of the surface charge of particles was calculated directly from the measured pH and acid or base added at each data point or by subtracting the oxide suspension titration curve from the curve corresponding to the background electrolyte in the absence of oxide. These two methods are based on the electroneutrality equation of the suspension. The surface charge density can thus be calculated for each data point as follows:

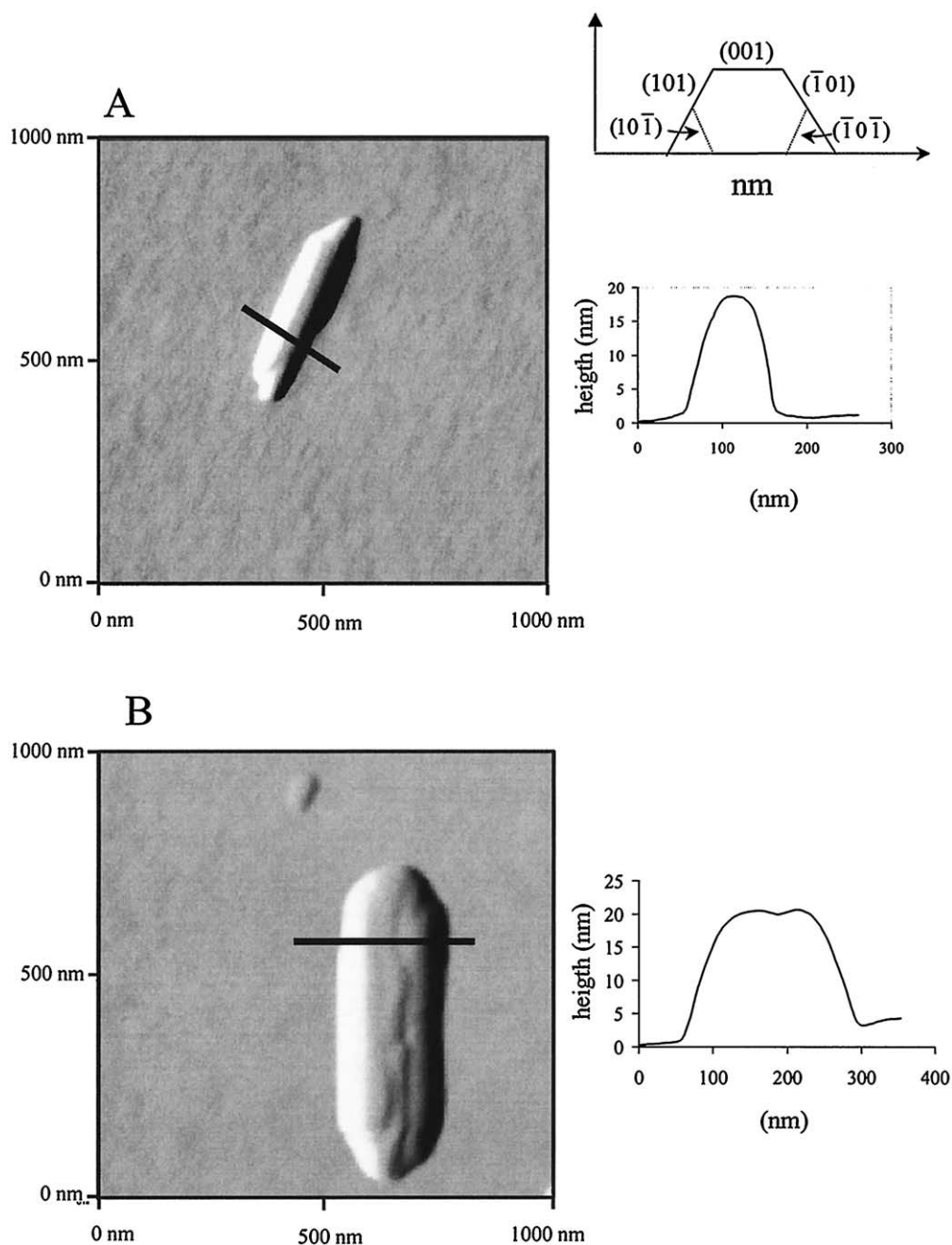


Fig. 1. Deflection mode images of two typical single G49 crystals. Seventy percent of the most common crystal type seen in (B) develop (001) faces. The z-profiles describe the height distributions along the lines shown within images.

$$\sigma = (F/A\rho)[C_A - C_B - [H^+] + [OH^-]], \quad (8)$$

or with the second method at each value of pH with

$$\sigma = (F/A\rho)[(C_A - C_B)_{\text{susp}} - (C_A - C_B)_{\text{blank}}], \quad (9)$$

where C_A and C_B are the concentrations of acid or base added to the suspension or blank, respectively, $[]$ is concentration of ions, F is Faraday's constant (96,480 C/mol of charge), A is the specific surface area (m^2/g), and ρ is the concentration of solid

(g/L). The same surface charge value was obtained regardless of the calculation method used.

To determine the charge on the basis of the electroneutrality equation, we must know the kinetic and thermodynamic reactivity of minerals in the studied pH range, in particular the dissolution of minerals and the adsorption of undesirable ions. In addition, the initial state of the suspension is very important for potentiometric experiments. Different procedures have been described for the preparation of samples for titration. Many authors washed the suspension or the freeze-dried product to

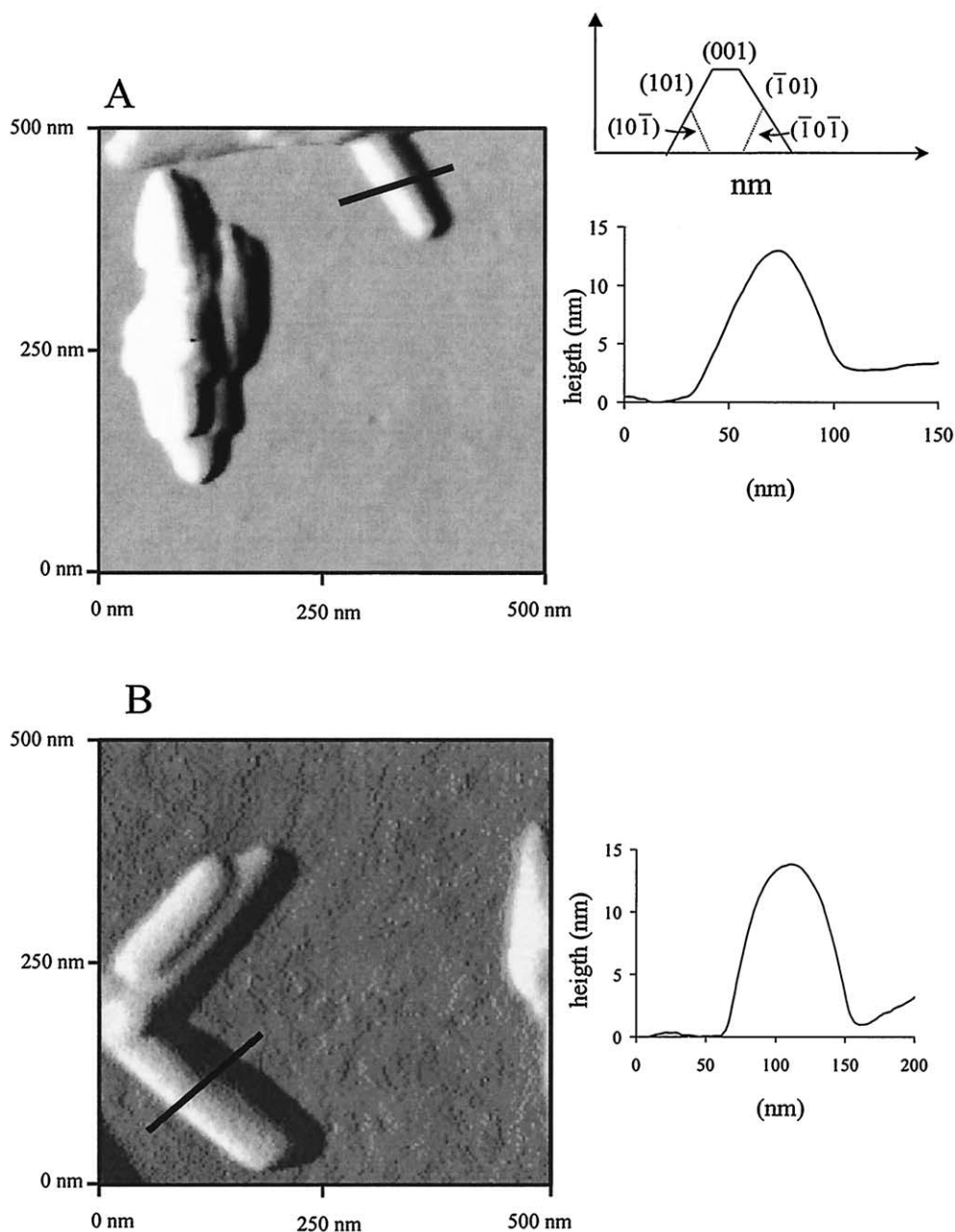


Fig. 2. Deflection mode images of two typical single G95 crystals. Thirty percent of the most common crystal type seen in (A) develop (001) faces. The z-profiles describe the height distributions along the lines shown within images.

remove impurities. Some authors dialyzed the produce against Milli-Q water, which is probably a more efficient method for the removal of salt ions from suspension and to equilibrate the suspension nearly to the zero surface charge. Other authors shifted the different curves such that the crossover point occurred at zero surface charge. As demonstrated previously, this shift is sometime due to insufficient quantity of solid in the titration reactor (Noh and Schwarz, 1989; Zalac and Kallay, 1992).

However, washing or dialysis with Milli-Q water (no carbonate, salt, or excess base or acid contamination) should ideally lead to the pH value of the suspension being equal to the

pzc value in the presence of salt (without the addition of acid or base). No studies have correctly looked at the effects of these different factors (e.g., suspension preparation, suspension concentration) on the determination surface charge by potentiometric titration.

3.2.2. Effect and Correction of the Carbonate Contamination

Figure 3 shows raw titration curve of one goethite suspension. The pH of the suspension was initially adjusted to approximately pH 4.0 (Fig. 3, open circles). The goethite suspension was then maintained in an argon atmosphere overnight

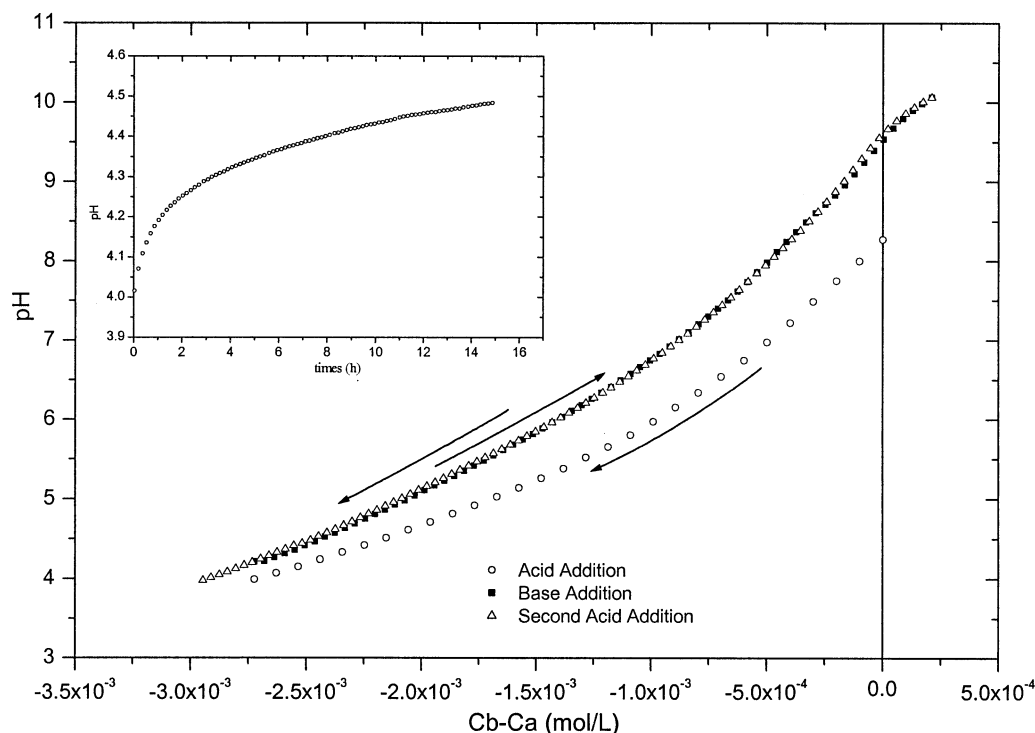


Fig. 3. Raw experimental data showing the effect of the concentration of total proton added on pH, i.e., base concentration (C_b) minus acid concentration (C_a), in the presence of a constant concentration of sodium nitrate ($\text{NaNO}_3 = 0.01 \text{ mol/L}$) for the G49 suspension. The inset shows how pH changed during the argon purge. The arrows represent the direction of the titration procedure (see text for more information).

(flux = 0.1 L/min), and changes in pH (Fig. 3, inset) were followed. The pH of the suspension was adjusted to pH 10 (Fig. 3, black squares), and a reverse titration was performed back to pH 4 (Fig. 3, open triangles). This titration procedure for the removal of carbonate ions from suspension was previously proposed by Hiemstra et al. (1996), but the raw data corresponding to the first acidification and pH change during purge were never shown or taken into account.

Our goethite suspensions were initially contaminated with carbonate ions, as confirmed by the hysteresis observed between the first acid addition (Fig. 3, open circles) and the two following additions (Fig. 3, black squares and open triangles) and the pH value at the beginning of the experiment (~ 8.2). Indeed, some authors have already suggested that this contamination occurs (Evans et al., 1979; Zeltner and Anderson, 1988; Lumsdon and Evans, 1994). These authors showed that the initial pHs of an unpurged goethite suspension and of a goethite suspension that had been purged with N_2 for 2 months were approximately 8.0 and 9.0, respectively. To avoid this drastic purge, we modified the procedure to account for this contamination in all experimental titrations.

The inset in Figure 3 shows how pH increases during an Ar purge. Proton ions are consumed because of the desorption and protonation of carbonate species that probably were eliminated from suspensions in dioxide gas. The pH did not increase during the Ar purge with the blank solution (no electrode drift). This demonstrates the strong affinity of carbonate ions for goethite surfaces.

However, the origin of the carbonate contamination needed

to be identified. The titration curves seen in Figure 3 correspond to the same goethite particles ($S = 49 \text{ m}^2/\text{g}$) as those studied by Leckie and coworkers, who concentrated on the adsorption of carbonate on the goethite surface (Van Geen et al., 1994; Villalobos and Leckie, 2000, 2001). They found that the pzc value of G49 is close to 9.0. As explained before, if no base or acid is added, the pH value of the suspension should correspond to the pzc value, in the absence of contamination. In our case, this value was close to 8.3, which confirms the presence of carbonate contamination. In fact, the only difference between our goethite preparation and that described by Leckie and coworkers is that they used boiled, high-purity (Milli-Q) water, whereas we used unboiled water for the dialysis step. We preferred to use unboiled water both for convenience and to avoid silica contamination from the Pyrex container used for boiling. Therefore, the sample probably becomes contaminated with carbonate during the dialysis procedure.

After removing the carbonate ions from suspension, no hysteresis was observed between the added base and the second acid titration curves (Fig. 3, black squares and open triangles). Because the surface charge was calculated from the concentrations of base and acid added ($C_b - C_a$), the consumption of proton ions during the Ar purge must be considered when calculating surface charge. The difference between the pH before and after the Ar purge was used to estimate the amount of protons consumed by the removed of carbonate ions. We used the Davies equation for the calculation of the activity coefficients at given concentrations to calculate the concentra-

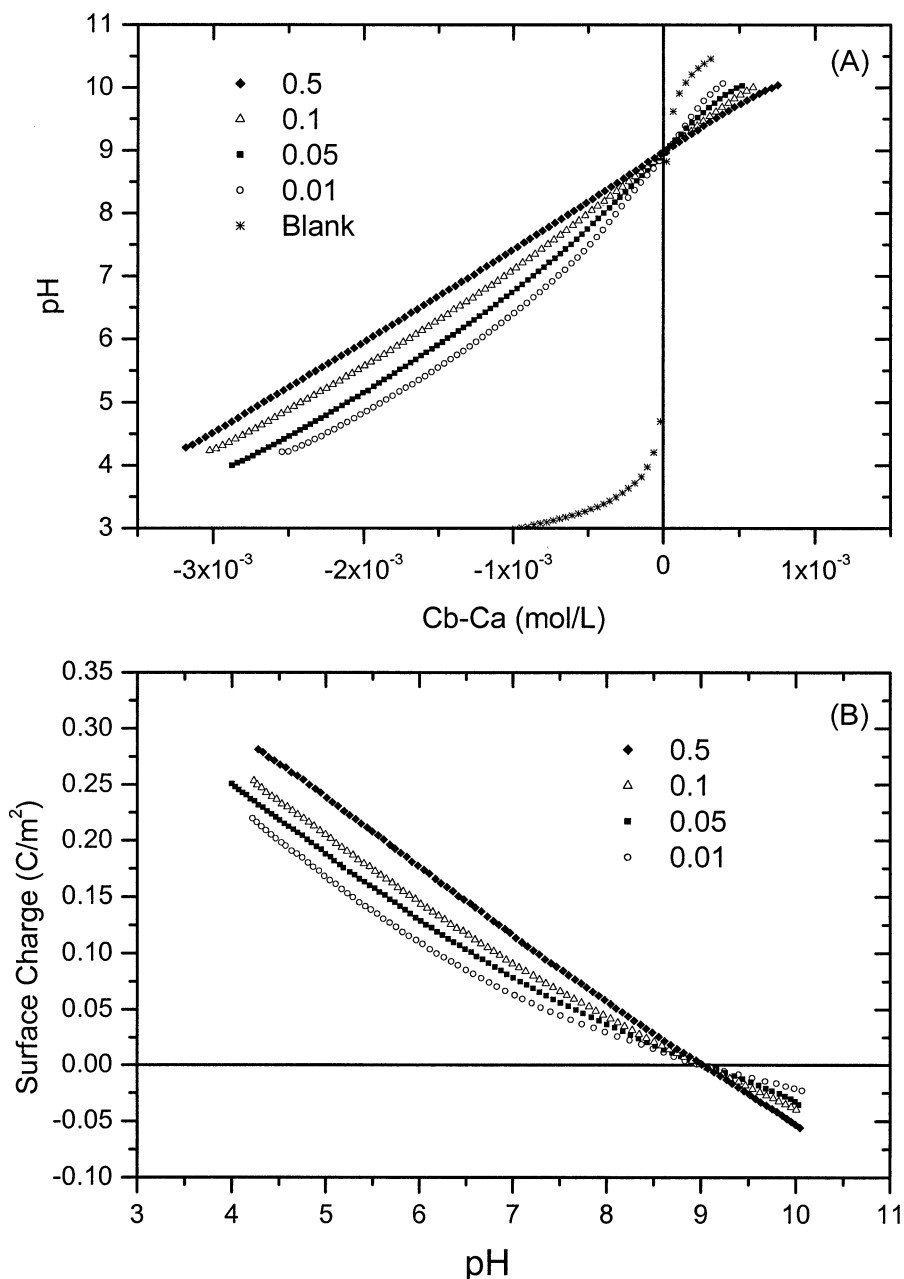


Fig. 4. (A) Raw experimental data showing the effect of the concentration of total proton added on pH, i.e., base concentration (C_b) minus acid concentration (C_a), at different concentrations of sodium nitrate (NaNO_3) for the G49 suspension. (B) The surface charge as calculated from the experimental data at four different electrolyte concentrations using the data from (A).

tion of protons taken up by the carbonate. This concentration was then added to each ($C_b - C_a$) value. Thus, for the goethite suspension shown in Figure 3, 7×10^{-5} mol/L of protons were consumed by the carbonate. This correction shifts the curve toward lower pH values. Indeed, the pH value corresponding to zero addition is now close to 9.0, while it previously crossed the zero abscissa at about pH 9.5. However, this carbonate correction resulted in a pH of zero surface charge (9.0) that was similar to that determined for the same type of goethite by Leckie and coworkers (Van Geen et al., 1994; Villalobos and

Leckie, 2000, 2001), which demonstrates the accuracy of this carbonate correction. This procedure was used to correct the raw data obtained with samples contaminated with carbonate before all of the surface charge calculations.

3.2.3. The Point-of-Zero Charge

Figures 4 and 5 show the corrected raw data and the surface charge curves for G49 and G95, respectively. The titration curves were similar for both goethites. Indeed, the surface

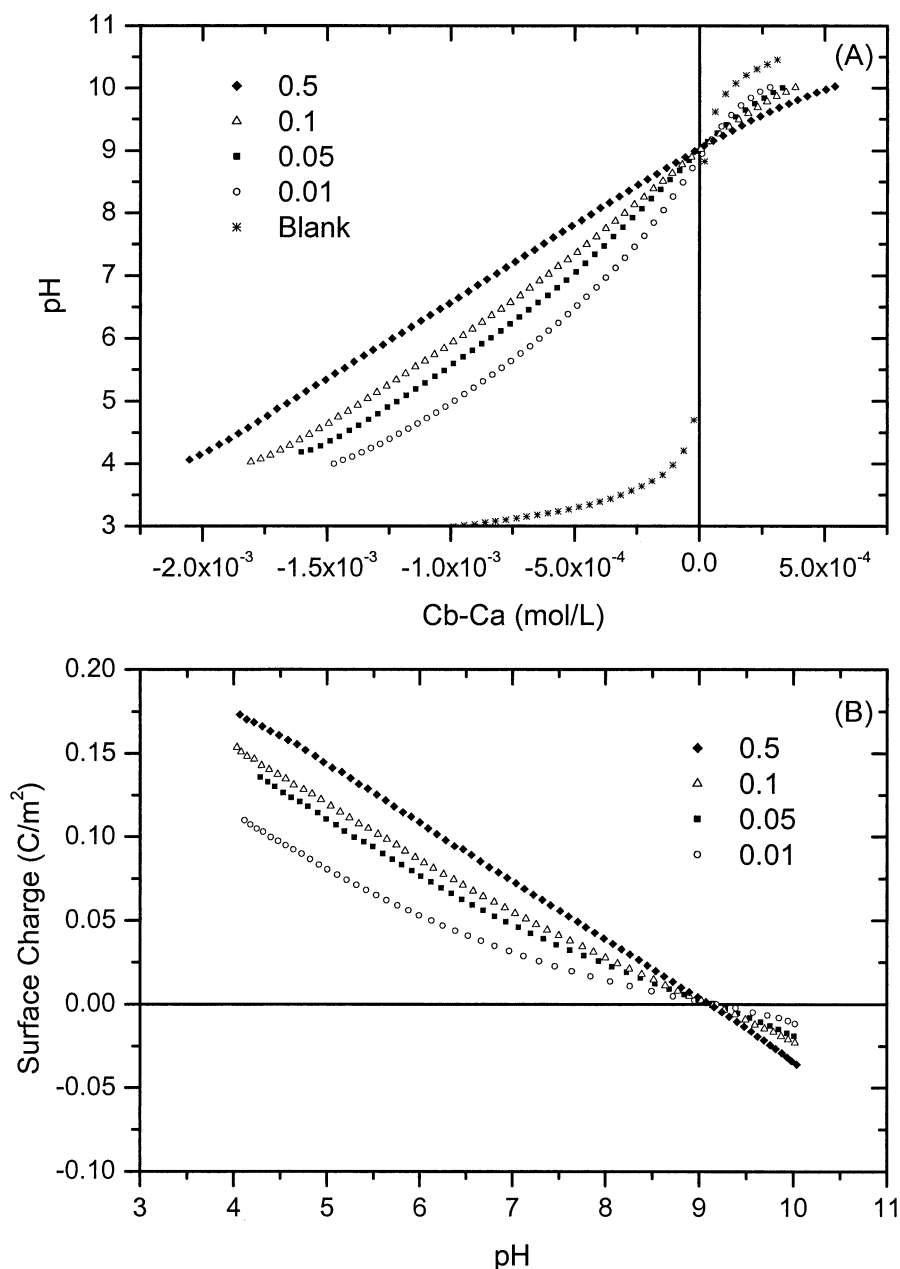


Fig. 5. (A) Raw experimental data showing how the concentration of total proton added affected pH, i.e., base concentration (C_b) minus acid concentration (C_a), at different concentrations of sodium nitrate (NaNO_3) for the G95 suspension. (B) The surface charge was calculated from the experimental data at four different electrolyte concentrations using the data from (A).

charge increases with concentration because the decrease of the apparent surface charge led to lower electrostatic repulsions, which enhanced the acid-base reactions on particle surfaces.

The common intersection point, which crosses the zero surface charge, between titration curves with different concentrations was used to define the zero point charge of the oxide particles. As shown by the raw data (top of Fig. 4 and Fig. 5), in both cases, this point corresponded to the zero surface charge. The pzc values obtained from our titration curves were 9.0 and 9.1 for G49 and G95, respectively. The accuracy of the pzc determination was estimated to be close to 0.05 from a set

of different experiments. Furthermore, the surface charge of G49 (Fig. 4) was higher than that of G95 (Fig. 5).

This is the first time that corrected acid-base titration data have been presented. This correction shifted the titration curves slightly toward a lower pH and probably corresponded to the shifts performed by some authors. The pzc value obtained for G49 (9.0) is consistent with results obtained by Leckie and coworkers (Van Geen et al., 1994; Villalobos and Leckie, 2000), demonstrating that our correction is correct. The carbonate correction yielded a pzc value of 9.1 for G95, which is slightly lower than the value reported for the same goethite by

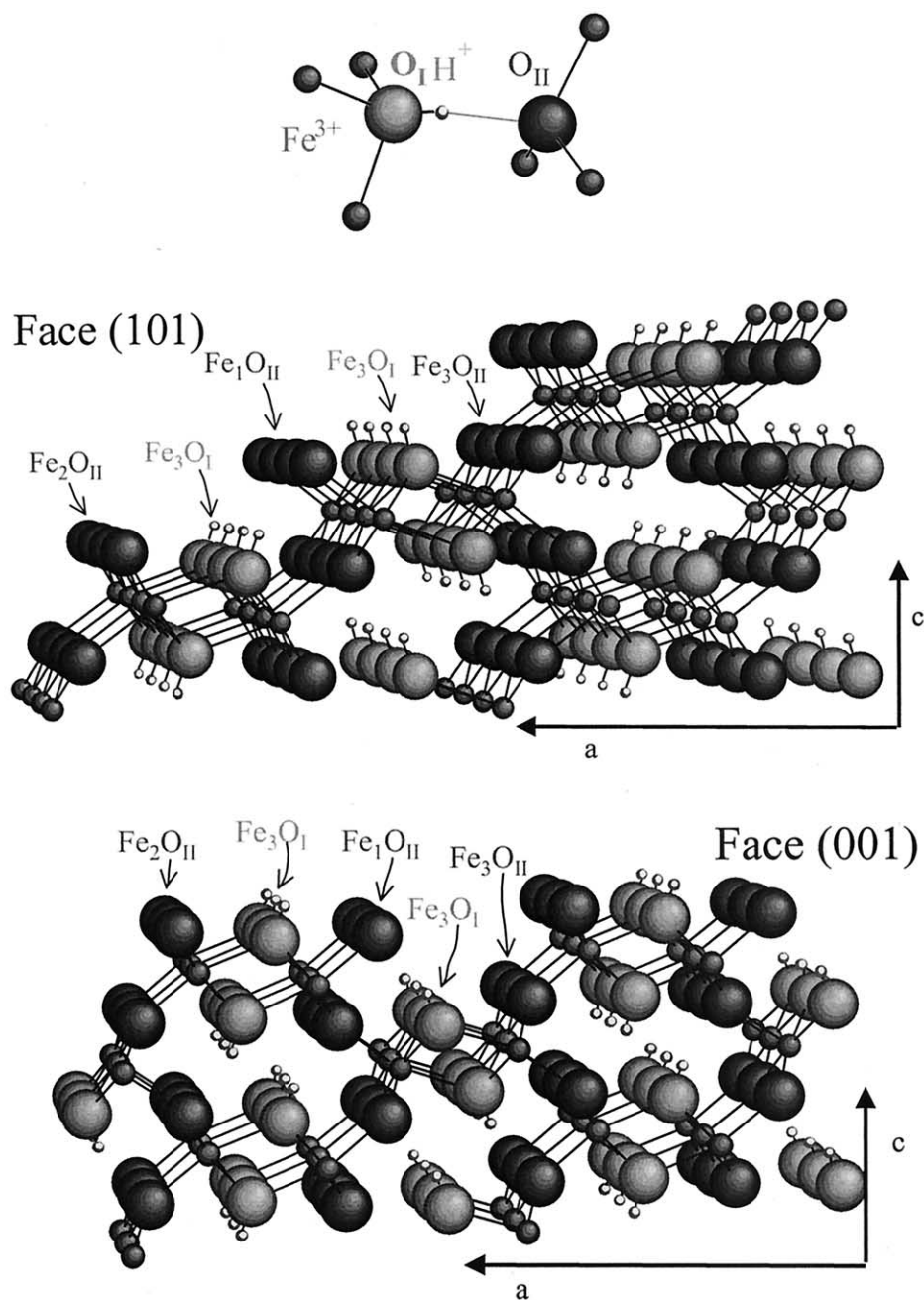


Fig. 6. Schematic representation of the surface structures of the (101) and (001) faces. The type of surface group is indicated according to the notation of Hiemstra et al. (1996).

Hiemstra and coworkers (9.3) (Rietra et al., 2000; Venema et al., 1996b, 1998). However, when we did not correct for carbonate contamination, we obtained a pzc value of 9.3, suggesting that these authors did not take this contamination into account. In addition, carbonate ion contamination would have occurred during dialysis because they also used double-distilled water rather than boiled water for this step.

The pzc values obtained for the two types of goethite affect the validity of the assumptions used for MUSIC predictions (Rietra et al., 2000; Venema et al., 1996b, 1998). Indeed, these authors predicted that the experimental pzc value would be

close to 9.3. However, the MUSIC calculation cannot explain the lower values obtained for goethite particles. We attempted to interpret these pzc values by use of the MUSIC approach, taking all of the hydrogen bond interactions between surface sites into account.

3.3. MUSIC Calculation

3.3.1. Multisite Approach

The use of Eqn. 1 and 2 to calculate proton affinity constants requires knowledge of the structure, the site density, and the

Table 1. Calculated proton affinities for the different surface groups of the (101) face of goethite according to the multisite complexation approach (Eq. 1 and 2). The dominant surface groups at the experimental pH range ($4 < \text{pH} < 10$) are indicated for each case.

	N_s (sites/nm ²)	s	$m + n$	m	n	Log $K_{i,1}$	Log $K_{i,2}$	Dominant
Fe ₃ O _I	6.06	0.411, 0.399, 0.399	1	0	1	11.7		Fe ₃ O _I H ^{+1/2}
Fe ₃ O _{II}	3.03	0.591, 0.610, 0.610	1	0	1	-0.2		Fe ₃ O _{II} ^{-1/2}
Fe ₂ O _{II}	3.03	A 0.591, 0.591	1	0, 1	1, 0	12.3	0.4	Fe ₂ O _{II} H ⁰
		B 0.591, 0.591	2	0, 1	2, 1	8.3	-3.6	Fe ₂ O _{II} ⁻¹ , Fe ₂ O _{II} H ⁰
Fe ₁ O _{II}	3.03	1 0.610	3	0, 1	3, 2	15.6	3.7	Fe ₁ O _{II} H ^{-1/2}
		2 0.610	2	0, 1	2, 1	19.6	7.7	Fe ₁ O _{II} H ₂ ^{+1/2} , Fe ₁ O _{II} H ^{-1/2}
		3 0.610	1	0, 1	1, 0	23.6	11.7	Fe ₁ O _{II} H ₂ ^{+1/2}

crystallographic distances of surface groups (Hiemstra et al., 1996). The AFM images (Fig. 1 and Fig. 2) demonstrated that (101) and/or (001) faces are always dominant on crystallized goethite. The vicinal (210) face was not considered because of its minor morphologic contribution on AFM images.

Goethite crystallizes in an orthorhombic system, with closely packed hexagonal arrays of oxygen atoms. According to the formula of goethite FeOOH, two different oxygens can be distinguished in goethite: a protonated oxygen (O_I) and an unprotonated oxygen (O_{II}) with a hydrogen bond (top of Fig. 6). Figure 6 shows the structure at the interface of the (101) and (001) faces of synthetic goethites. As demonstrated previously, four types of surface group are present on these faces (Hiemstra et al., 1996; Weidler et al., 1998).

The proton affinity constant of each surface group was systematically calculated according to the number of donating and/or accepting H bonds exchanged, i.e., $m + n$. Tables 1 and 2 present the results of these calculations for the two (101) and (001) faces, respectively. The bond valence, s , in these tables was calculated from Eqn. 2 with bond lengths ($R_{i,j}[s]$) of 1.958 Å (0.591) for type I oxygen and 1.946 Å (0.610) for type II oxygen. Hiemstra et al. (1996) previously calculated bond lengths of 2.092 Å (0.411) and 2.103 Å (0.399) for the two oxygen types, respectively.

For the triply coordinated groups (Fe₃O_I and Fe₃O_{II}), only one accepting hydrogen bond is possible, i.e., $m + n = 1$. In addition, because the Fe-O bonds for these two surface groups are the same length for the (001) and (101) faces, the proton affinity constants are also the same. Despite this similarity, the site density of these surface groups (Fe₃O_I and Fe₃O_{II}) is different on the faces considered here, which results in different contributions to the surface charge.

For the doubly and singly coordinated groups (Fe₂O_{II} and Fe₁O_{II}), different numbers of donating or accepting hydrogen

bonds, i.e., $m + n$, can be considered. Hiemstra and coworkers (Hiemstra et al., 1996; Venema et al., 1998) considered, for steric reasons on the (101) face calculation, that singly coordinated groups interact with only two donating or accepting hydrogen bonds ($m + n = 2$), whereas doubly coordinated groups interact with only one hydrogen bond ($m + n = 1$). When they applied this assumption to the calculation of the charge of the (101) face, the pzc value was 9.5. (Hiemstra et al., 1996). This specific situation corresponds to the A2 case mentioned in Table 1. Even if we consider that this value is reasonably similar to the experimental values found in our work (9.0 and 9.1), we decided to further the assumptions of this model to explain these lower values. In addition, this prediction means that a (001) face would have a pzc value identical to that of the (101) face, 9.5 (case C2, Table 2).

The proton affinity constants of other cases were considered to test the validity of this assumption and the effect of the accepting and donating hydrogen bonds on the shape of the curves and on the pzc value. We also performed this calculation for the (001) face, which is predominant in low-surface area goethite and has never been done with the current version of MUSIC (Hiemstra et al., 1996).

The charging curves for the six different situations were calculated for each face (101) and (001) considering the different values of donating and accepting hydrogen bonds. Figure 7 shows how the surface charge changes with pH, as calculated from the proton affinity constants shown in Table 1 for the (101) face. It is clear that surface charge is strongly dependent on the number of accepting and donating hydrogen bonds considered. The pzc values obtained from these curves vary from 6.0 to 11.2. In addition, the mean charge curve, obtained from the average contribution of each case, had a pzc value of 9.2.

Figure 8 shows how the surface charge changes with pH, as

Table 2. Calculated proton affinities for the different surface groups of the (001) face of goethite according to the multisite complexation approach (Eqn. 1 and 2). The dominant surface groups at the experimental pH range ($4 < \text{pH} < 10$) are indicated for each case.

	N_s (sites/nm ²)	s	$m + n$	m	n	Log $K_{i,1}$	Log $K_{i,2}$	Dominant
Fe ₃ O _I	6.68	0.411, 0.399, 0.399	1	0	1	11.7		Fe ₃ O _I H ^{+1/2}
Fe ₃ O _{II}	3.34	0.591, 0.610, 0.610	1	0	1	-0.2		Fe ₃ O _{II} ^{-1/2}
Fe ₂ O _{II}	3.34	C 0.610, 0.610	1	0, 1	1, 0	11.5	-0.4	Fe ₂ O _{II} H ⁰
		D 0.610, 0.610	2	0, 1	2, 1	7.5	-4.3	Fe ₂ O _{II} ⁻¹ , Fe ₂ O _{II} H ⁰
Fe ₁ O _{II}	3.34	1 0.591	3	0, 1	3, 2	16.0	4.1	Fe ₁ O _{II} H ^{-1/2}
		2 0.591	2	0, 1	2, 1	19.9	8.0	Fe ₁ O _{II} H ₂ ^{+1/2} , Fe ₁ O _{II} H ^{-1/2}
		3 0.591	1	0, 1	1, 0	23.9	12.0	Fe ₁ O _{II} H ₂ ^{+1/2}

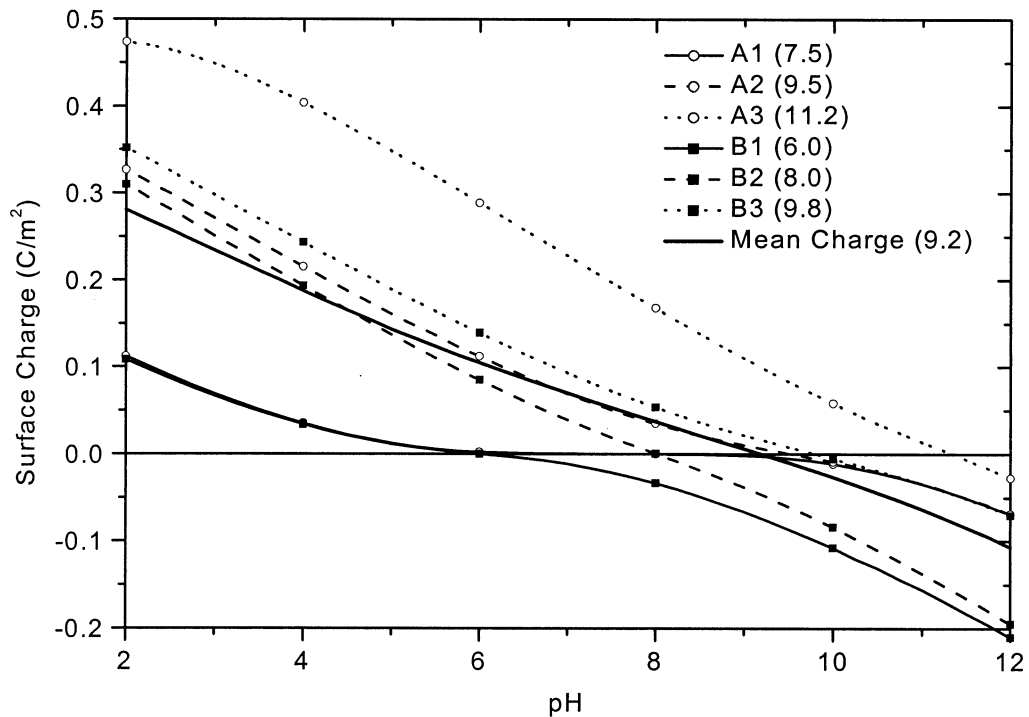


Fig. 7. The calculated surface charge of the (101) face of goethite vs. pH for the different cases considered in Table 1. For each curve, the acid-base equilibrium and the constants (Table 1) of the two types of triply coordinated group, of the doubly coordinated groups (A or B), and of the singly coordinated groups (1, 2, or 3) were considered.

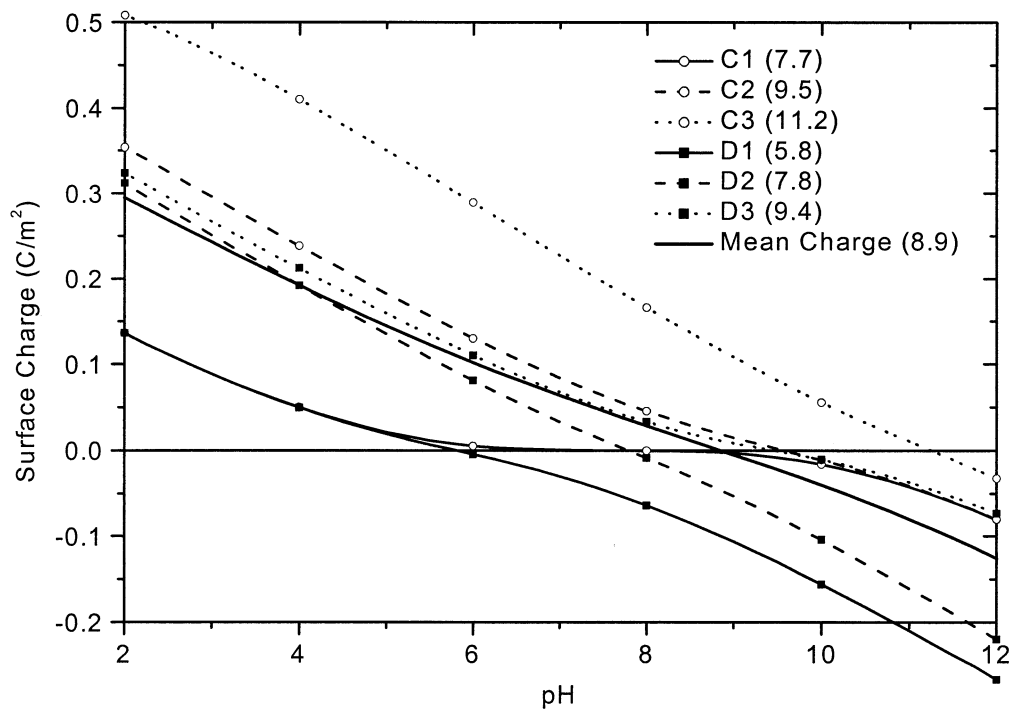


Fig. 8. The calculated surface charge of the (001) face of goethite vs. pH for the different cases considered in Table 2. For each curve, the acid-base equilibrium and the respective constants (Table 2) of triply coordinated group, of the doubly coordinated groups (A or B), and of the singly coordinated groups (1, 2, or 3) were considered.

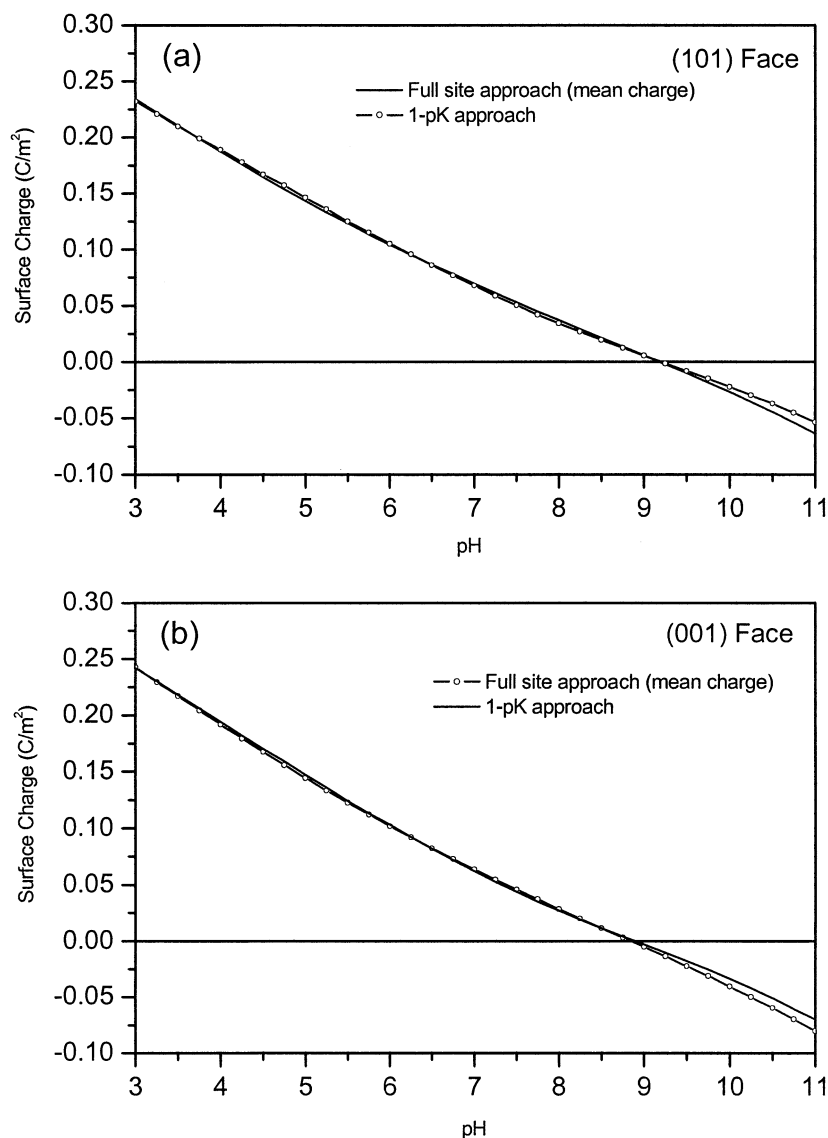


Fig. 9. Comparison of the charging curves for the mean charge curve obtained by use of the full-site approach and by use of the simplified 1-pK approach in 0.1-mol/L NaNO_3 for both (a) (101) and (b) (001) faces. In all cases, we assumed that the ion pair forms symmetrically ($\text{Log}K_C = \text{Log}K_A = -1$). For the 1-pK calculation, the surface density and the proton affinity constants were set to (a) $N_s = 6.06$ sites/ nm^2 , $\text{Log}K_H = 9.2$, and (b) $N_s = 6.68$ sites/ nm^2 , $\text{Log}K_H = 8.9$. The resulting Stern capacitances for the 1-pK calculation were (a) 0.9 F/m^2 and (b) 1.0 F/m^2 .

calculated from the proton affinity constants shown in Table 2 for the (001) face. The same trends were obtained for this face, demonstrating that the donating and accepting hydrogen bonds had a strong effect on the surface charge curves. The pzc values for the different situations were between 5.8 and 11.2, and the pzc value of the mean charge curve deduced from these curves was 8.9, which is lower than on the (101) face.

The experimental pzc values obtained for G49 (pzc = 9.0) and G95 (pzc = 9.1) goethite suspensions were situated between the two theoretical pzc values calculated for the two faces: (001), pzc = 8.9; and (101), pzc = 9.2. The morphologic description obtained from AFM images further suggests that the experimental pzc value increases together with the number of (101) faces. In fact, if we assume a linear relationship

between the individual pzc value of the two faces and the area percentage of (001) face, the experimental values obtained for G49 (pzc = 9.0, 70% (001), 30% (101)) and for G95 (pzc = 9.1, 30% (001), 70% (101)) lie exactly on the theoretical line that passes through the two theoretical values, i.e., pzc = 8.9, % (001) = 100; and pzc = 9.2, % (001) = 0.

These results demonstrate that the static description of each case is probably not a realistic description of the interface and that the Hiemstra and coworkers' hypothesis, which only considers A2 or C2 (Table 1 and Table 2) for steric reasons, is too restrictive and ambiguous (Hiemstra et al., 1996; Venema et al., 1998). Indeed, this specific situation leads to the same theoretical pzc value for the (001) and (101) faces (9.5), which disagrees with our experimental values.

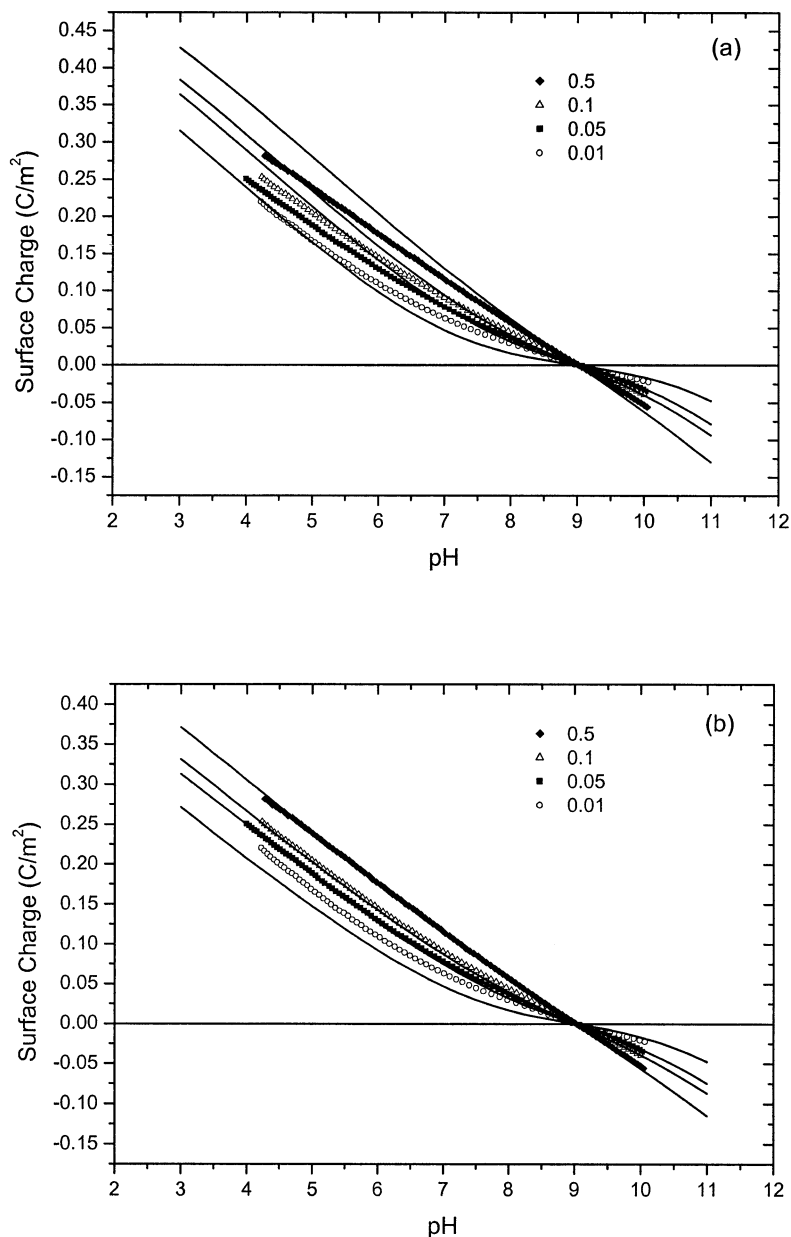


Fig. 10. Charging behavior of G49 in the presence of different concentrations of NaNO_3 . The lines represent the model calculations, and the dots represent data from Figure 4B. For the two calculations, we assumed that ion pairs formed symmetrically ($\text{Log}K_c = \text{Log}K_A = -1$), and the proton affinity constants were set to $\text{Log}K_H = 9.0$. The surface density and Stern capacitances used were (a) $N_s = 6.50$ sites/ nm^2 , $C_s = 1.8$ F/ m^2 , and (b) $N_s = 12$ sites/ nm^2 , $C_s = 1.3$ F/ m^2 .

3.3.2. 1-pK Approach

In the multisite approach, the theoretical pzc values, which were derived from the mean charge curve of the six different situations, were found to correspond to the experimental ones and the face distributions of goethite particles. This result demonstrates that face distributions have a small effect on the experimental pzc values, i.e., G49 (pzc = 9.0, 70% (001), 30% (101) and G95 (pzc = 9.1, 30% (001)). To validate this theoretical description, experimental surface charges need to be compared with theoretical ones.

These multisite calculations resulted from the mean charge of the different contributions. Therefore, it is easier to optimize the free parameters for a best fitting model with a much simpler model, such as 1-pK. In addition, the proton affinity constant of this single equilibrium (5) was set to the experimental pzc value, whereas in the multisite approach, there is little difference between the experimental and the theoretical values. However, this simplification always requires that this multisite approach be compared with the 1-pK calculation.

In the case of a basic Stern model, the 1-pK approximation

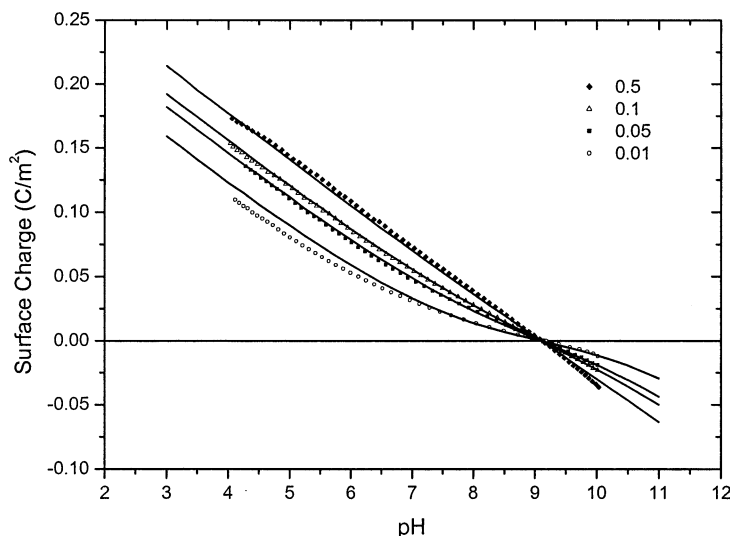
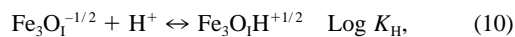


Fig. 11. Charging behavior of G95 in the presence of different concentrations of NaNO_3 . The lines represent the model calculations, and the dots represent data from Figure 5B. For the two calculations, we assumed that ion pairs were formed symmetrically ($\text{Log}K_C = \text{Log}K_A = -1$), and the proton affinity constants were set to $\text{Log}K_H = 9.1$. The surface density and Stern capacitance used were $N_s = 6.24$ sites/ nm^2 , $C_s = 0.73$ F/ m^2 .

only makes it possible to optimize the Stern capacitance, the ion pair formation constant, and the surface site density. To reduce the number of free parameters, Hiemstra et al. (1996) estimated the surface site density from crystallographic data and cancelled some of the surface site contributions from the multisite approach predictions. Therefore, the latter assumption is based on the calculation of the proton affinity constants, which consider only one specific situation for interaction between the hydrogen bonds and the surface site, i.e., case A2 (Table 1) for (101) faces and case C2 (Table 2) for (001) faces. This simplification cancels out the contribution of the doubly coordinated groups, which is neutral at pH 2 to 11, and considers only triply coordinated Fe_3O_I groups with a surface site density of 3.03 and 3.34 for the (101) and (001) faces, respectively, because of the constant negative contribution of the Fe_3O_{II} to the charge balance of the system. This assumption implies that the 1-pK equilibrium (5) represents the sum of the two following protonation equilibria with the same affinity constant:



On the basis of these considerations, the mean curve of the full-site approach for both faces was fitted with the 1-pK approach, using only the Stern capacitance as a free parameter. Figure 9 depicts the result of these calculations for the (101) and (001) faces. There is a very good agreement between these two approaches, demonstrating the accuracy of the simpler 1-pK model for the description of the mean curve of the full site approach. Therefore, the 1-pK approach can be used to quantify the charging properties of our two goethites.

Because the goethite particles present two different faces, the face distributions obtained with the AFM method were required to calculate the surface sites density. G49 exhibited a face

distribution of 70% (001) and 30% (101), which leads to 6.50 sites/ nm^2 . G95 exhibited a face distribution of 30% (001) and 70% (101), giving 6.24 sites/ nm^2 . The best fitting of 1-pK calculations are plotted against the experimental data in Figures 10 and 11 for G49 and G95, respectively.

The first calculation performed with crystallographic surface density ($N_s = 6.50$ sites/ nm^2) and the experimental data for G49 (Fig. 10a) fitted poorly and had a higher Stern capacitance ($C_s = 1.8$ F/ m^2). This significant deviation could not be corrected by changing the symmetrical ion pair formation, but could be corrected by increasing the surface site density. This calculation was then repeated with a higher surface site density ($N_s = 12.0$ sites/ nm^2) (Fig. 10b), leading to reasonable agreement between the calculated and the experimental charging curves. However, one set of parameters led to a reasonable description of the titration data in both of these two situations. This significant deviation (Fig. 10a) resulted from the predictions of proton affinity constants according to the method of Hiemstra et al. (1996) (cases A2 and C2), which cancelled some surface site contributions; thus, it is probably not realistic. Conversely, the 1-pK approximation fitted reasonably well with the titration data of G95, when using the active surface site density as estimated from crystallographic data and MUSIC predictions (cases A2 and C2).

The significant differences between the charging behaviors of the two goethites studied do not imply significant differences in pzc values. Indeed, a high surface site density and Stern capacitance ($N_s = 12$ sites/ nm^2 , $C_s = 1.3$ F/ m^2) are required to describe the experimental charging data for G49, whereas much smaller ones ($N_s = 6.24$ sites/ nm^2 , $C_s = 0.73$ F/ m^2) are required for G95, which is in agreement with the estimated surface site density. Boily et al. (2000) suggested that surface roughness and edge surface sites could enhance surface site densities.

4. CONCLUSION

We provide experimental data on both crystal morphology and surface charging behavior. These results demonstrate that surface charge value depends upon the morphology of particles, i.e., the crystalline faces distribution, while pzc values are slightly influenced. The experimental pzc values of two types of goethite (49 m²/g, pzc = 9.0; 95 m²/g, pzc = 9.1) were similar to the theoretical values obtained by MUSIC calculations using the full-site approach. However, these results must be interpreted with care, as we have not yet demonstrated that the interfaces described by the MUSIC model hold true in real conditions. The formalism of the reaction is a good way to improve surface complexation modeling, but the predicted proton affinity constants must be interpreted carefully.

In fact, the much simpler 1-pK approach better describes the titration data with only two or three free parameters, which could be a serious constraint. These calculations demonstrate the usefulness of single-site approach to reproduce experimental curves. The surface site density deduced from the estimation of affinity constant from the MUSIC model agrees for one type of goethite, while higher value is required for the other one (G49) to fit well experimental curves.

However, the multisite approach could not explain the differences in surface charge between the two goethites that demonstrate its limitation. These theoretical considerations can undoubtedly be improved because some discrepancy still exists in the way to predict and describe the acid-base properties of oxide. Indeed, large differences in affinity constants exist between the surface groups of goethite determined from MUSIC calculations and from molecular dynamics (Felmy and Rustad, 1998; Rustad et al., 1996a, 1996b). However, the discrimination between these different approaches requires more experimental investigation, which leads to local description of face reactivity. For example, these theoretical studies should be completed by experimental investigations using surface force measurement by AFM to measure the local surface charges of the individual crystalline faces (Eggleston and Jordan, 1998; Finot et al., 2000).

Acknowledgments—The authors are grateful to the CNRS for the financial support they received from the PRACIS GdR program and the ACI X6 “Eau et Environnement” grant from the INSU-CNRS, 2001 to 2003. We thank M. Abdelmoula (LCPME, Villers-lès-Nancy) for carrying out the Mössbauer spectroscopy experiments and M. Paris (ESSTIN, Nancy) for carrying out the X-ray diffraction analyses. Thanks are also due to F. Ait-Mesbah for her contribution to the potentiometric titrations. Finally, we would like to thank D. A. Sverjensky, W. H. Van Riemsdijk, and two anonymous reviewers for their constructive comments.

Associate editor: D. A. Sverjensky

REFERENCES

- Atkinson F. J., Posner A. M., and Quirk J. P. (1967) Adsorption of Potential determining ions at the ferric oxide-aqueous electrolyte interface. *J. Phys. Chem.* **71**, 550–558.
- Boily J.-F., Nilsson N., Persson P., and Sjöberg S. (2000) Benzenecarboxylate surface complexation at the goethite (FeOOH)/water interface: I. A mechanistic description of pyromellitate surface complexes from the combined evidence of infrared spectroscopy, potentiometry, adsorption data, and surface complexation modeling. *Langmuir* **16**, 5719–5729.
- Boily J.-F., Lützenkirchen J., Balmès O., Beattie J., and Sjöberg S. (2001) Modeling proton binding at the goethite (α -FeOOH)-water interface. *Colloids Surf., A: Physicochem. Eng. Aspects* **179**, 11–27.
- Bourikas K., Hiemstra T., and Van Riemsdijk W. H. (2001) Ion pair formation and primary charging behavior of titanium oxide (anatase and rutile). *Langmuir* **17**, 749–756.
- Charmas R. (1999) Four-layer complexation model for ion adsorption at energetically heterogeneous metal oxide/electrolyte interfaces. *Langmuir* **15**, 5635–5648.
- Contescu C., Popa V. T., and Schwarz J. A. (1996) Heterogeneity of hydroxyl and deuteroyl groups on the surface of TiO₂ polymorphs. *J. Colloid Interface Sci.* **180**, 149–161.
- Cornell R. M. and Schwertmann U. (1996) *The Iron Oxides: Structure, Properties, Reactions, Occurrence and Uses*. VCH, New York.
- Davis J. A. and Leckie J. O. (1978a) Speciation of adsorbed ions at the oxide/water interface. In *Chemical Modeling in Aqueous Systems*, pp. 299–317.
- Davis J. A. and Leckie J. O. (1978b) Surface ionization and complexation at the oxide/water interface. II. Surface properties of amorphous iron oxyhydroxide and adsorption of metal ions. *J. Colloid Interface Sci.* **67**, 90–107.
- Dzombak D. and Morel F. (1990) *Surface Complexation Modeling*. John Wiley, New York.
- Eggleston C. M. and Jordan G. (1998) A new approach to pH of point of zero charge measurement: Crystal-face specificity by scanning force microscopy (SFM). *Geochim. Cosmochim. Acta* **62**, 1919–1923.
- Evans T. D., Leal J. R., and Arnold P. W. (1979) The interfacial electrochemistry of goethite (α -FeOOH), especially the effect of CO₂ contamination. *J. Electro. Chem.* **105**, 161–167.
- Felmy A. R. and Rustad J. R. (1998) Molecular statics calculations of proton binding to goethite surfaces: Thermodynamic modeling of the surface charging and protonation of goethite in aqueous solution. *Geochim. Cosmochim. Acta* **62**, 25–31.
- Finot E., Lesniewska E., Mutin J.-C., and Goudonnet J.-P. (2000) Investigations of surface forces between gypsum microcrystals in air using atomic force microscopy. *Langmuir* **16**, 4237–4244.
- Hahn T., ed. (1996) *International Tables of Crystallography*. Kluwer Academic Publishers, Norwell, MA.
- Hayes K. F. and Leckie J. O. (1987) Modeling ionic strength effects on cation adsorption at hydrous oxide/solution interfaces. *J. Colloid Interface Sci.* **115**, 564–572.
- Hayes K. F., Papelis C., and Leckie J. O. (1988) Modeling ionic strength effects on anion adsorption at hydrous oxide/solution interfaces. *J. Colloid Interface Sci.* **125**, 717–726.
- Hayes K. F., Redden G., Ela W., and Leckie J. O. (1991) Surface complexation models: An evaluation of model parameter estimation using FITEQL and oxide mineral titration data. *J. Colloid Interface Sci.* **142**, 448–469.
- Hiemenz P. C. (1977) *Principle of Colloid and Surface Chemistry*. Marcel Dekker, New York.
- Hiemstra T. and Van Riemsdijk W. H. (1996) A surface structural approach to ion adsorption: The charge distribution (CD) model. *J. Colloid Interface Sci.* **179**, 488–508.
- Hiemstra T. and Van Riemsdijk W. H. (1999a) Effect of different crystal faces on experimental interaction force and aggregation of hematite. *Langmuir* **15**, 8045–8051.
- Hiemstra T. and Van Riemsdijk W. H. (1999b) Surface structural ion adsorption modeling of competitive binding of oxyanions by metal (hydr)oxides. *J. Colloid Interface Sci.* **210**, 182–193.
- Hiemstra T., Van Riemsdijk W. H., and Bruggenwert M. G. (1987) Proton adsorption mechanism at the gibbsite and aluminium oxide solid/solution interface. *Netherlands J. Agricultural Sci.* **35**, 281–293.
- Hiemstra T., De Wit J. C. M., and Van Riemsdijk W. H. (1989a) Multisite proton adsorption modeling at the solid/solution interface of (hydr)oxides: A new approach. II. Application to various important (hydr)oxides. *J. Colloid Interface Sci.* **133**, 105–117.
- Hiemstra T., Van Riemsdijk W. H., and Bolt G. H. (1989b) Multisite proton adsorption modeling at the solid/solution interface of (hydr)oxides: A new approach. I. Model description and evaluation of intrinsic reaction constants. *J. Colloid Interface Sci.* **133**, 91–104.

- Hiemstra T., Venema P., and Van Riemsdijk W. H. (1996) Intrinsic proton affinity of reactive surface groups of metal (hydr)oxides: The bond valence principle. *J. Colloid Interface Sci.* **184**, 680–692.
- Hochella M. F. and White A. F., eds. (1990) *Mineral-Water Interface Geochemistry, Vol. 23*. Mineralogical Society of America, Washington, DC.
- Hsi C.-K. D. and Langmuir D. (1985) Adsorption of uranyl onto ferric oxyhydroxides: Application of the surface complexation site-binding model. *Geochim. Cosmochim. Acta* **49**, 1931–1941.
- Israelachvili J. (1992) *Intermolecular & Surface Forces*. Academic Press, San Diego, CA.
- Keizer M. G. and Van Riemsdijk W. H. (1994) *ECOSAT: Technical Report of the Departments of Soil Science and Plant Nutrition*. Wageningen Agricultural University, Wageningen, the Netherlands.
- Lövgren L., Sjöberg S., and Schindler P. W. (1990) Acid/base reactions and Al(III) complexation at the surface of goethite. *Geochim. Cosmochim. Acta* **54**, 1301–1306.
- Lumsdon D. G. and Evans L. J. (1994) Surface complexation model parameters for goethite (α -FeOOH). *J. Colloid Interface Sci.* **164**, 119–125.
- Magonov S. N. and Whangbo M.-H. (1996) *Surface Analysis With STM and AFM: Experimental and Theoretical Aspects of Image Analysis*. VCH, New York.
- Nabavi M., Spalla O., and Cabane B. (1993) Surface chemistry of nanometric ceria particles in aqueous dispersions. *J. Colloid Interface Sci.* **160**, 459–471.
- Noh J. S. and Schwarz J. A. (1989) Estimation of the point of zero charge of simple oxides by mass titration. *J. Colloid Interface Sci.* **130**, 157–164.
- Parks G. A. and De Bruyn P. L. (1962) The zero point of charge of oxides. *J. Phys. Chem.* **66**, 967–973.
- Pauling L. (1929) The principles determining the structure of complex ionic crystals. *J. Am. Chem. Soc.* **51**, 1010.
- Rietra R. P., Hiemstra T., and Van Riemsdijk W. H. (1999a) Sulfate adsorption on goethite. *J. Colloid Interface Sci.* **218**, 511–521.
- Rietra R. P., Hiemstra T., and Van Riemsdijk W. H. (1999b) The relationship between molecular structure and ion adsorption on variable charge minerals. *Geochim. Cosmochim. Acta* **63**, 3009–3015.
- Rietra R. P., Hiemstra T., and Van Riemsdijk W. H. (2000) Electrolyte anion affinity and its effect on oxyanion adsorption on goethite. *J. Colloid Interface Sci.* **229**, 199–206.
- Robertson A. P. and Leckie J. O. (1997) Cation binding predictions of surface complexation models: Effects of pH, ionic strength, cation loading, surface complex, and model fit. *J. Colloid Interface Sci.* **188**, 444–472.
- Rudzinski W., Charnas R., and Piasecki W. (1999) Searching for thermodynamic relations in ion adsorption at oxide/electrolyte interfaces studied by using the 2-pK protonation model. *Langmuir* **15**, 8553–8557.
- Rustad J. R., Felmy A., and Hay B. P. (1996a) Molecular statics calculations for iron oxide and oxyhydroxide minerals: Toward a flexible model of the reactive mineral-water interface. *Geochim. Cosmochim. Acta* **60**, 1553–1562.
- Rustad J. R., Felmy A., and Hay B. P. (1996b) Molecular statics calculations of proton binding to goethite surfaces: A new approach to estimation of stability constants for multisite surface complexation models. *Geochim. Cosmochim. Acta* **60**, 1563–1576.
- Schwertmann U., Cambier P., and Murad E. (1985) Properties of goethites of varying crystallinity. *Clays Clay Mineral.* **33**, 369–378.
- Sparks D. L. and Grundl T. J., eds. (1999) *Mineral-Water Interfacial Reactions, Kinetics and Mechanisms*. ACS Symposium Series No. 715. American Chemical Society, Washington, DC.
- Sposito G. (1984) *The Surface Chemistry of Soils*. Oxford University Press, New York.
- Sposito G. (1998) On points of zero charge. *Environ. Sci. Technol.* **32**, 2815–2819.
- Strauss R., Brümmer G. W., and Barrow N. J. (1997a) Effects of crystallinity of goethite: I. Preparation and properties of goethites of differing crystallinity. *Eur. J. Soil Sci.* **48**, 87–99.
- Strauss R., Brümmer G. W., and Barrow N. J. (1997b) Effects of crystallinity of goethite: II. Rates of sorption and desorption of phosphate. *Eur. J. Soil Sci.* **48**, 101–114.
- Stumm W. (1992) *Chemistry of the Solid-Water Interface*. John Wiley, New York.
- Sverjensky D. A. and Sahai N. (1996) Theoretical prediction of single-site surface-protonation equilibrium constants for oxides and silicates in water. *Geochim. Cosmochim. Acta* **60**, 3773–3797.
- Van Geen A., Robertson A. P., and Leckie J. O. (1994) Complexation of carbonate species at the goethite surface: Implications for adsorption of metal ions in natural waters. *Geochim. Cosmochim. Acta* **58**, 2073–2086.
- Van Riemsdijk W. H., De Wit J. C. M., Koopal L. K., and Bolt G. H. (1987) Metal ion adsorption on heterogeneous surfaces: adsorption models. *J. Colloid Interface Sci.* **116**, 511–522.
- Venema P., Hiemstra T., and Van Riemsdijk W. H. (1996a) Comparison of different site binding models for cation sorption: Description of pH dependency, salt dependency, and cation-proton exchange. *J. Colloid Interface Sci.* **181**, 45–59.
- Venema P., Hiemstra T., and Van Riemsdijk W. H. (1996b) Multisite adsorption of cadmium on goethite. *J. Colloid Interface Sci.* **183**, 515–527.
- Venema P., Hiemstra T., Weidler P. G., and Van Riemsdijk W. H. (1998) Intrinsic proton affinity of reactive surface groups of metal (hydr)oxides: Application to iron (hydr)oxides. *J. Colloid Interface Sci.* **198**, 282–295.
- Villalobos M. and Leckie J. O. (2000) Carbonate adsorption on goethite under closed and open CO₂ conditions. *Geochim. Cosmochim. Acta* **64**, 3787–3802.
- Villalobos M. and Leckie J. O. (2001) Surface complexation modeling and FTIR study of carbonate adsorption to goethite. *J. Colloid Interface Sci.* **235**, 15–32.
- Weidler P. G., Schwinn T., and Gaub H. E. (1996) Vicinal faces on synthetic goethite observed by atomic force microscopy. *Clays Clay Mineral* **44**, 437–442.
- Weidler P. G., Hug S. J., Wetche T. P., and Hiemstra T. (1998) Determination of growth rates of (100) and (110) faces of synthetic goethite by scanning force microscopy. *Geochim. Cosmochim. Acta* **62**, 3407–3412.
- Wiesendanger R. (1994) *Scanning Probe Microscopy and Spectroscopy: Methods and Applications*. Cambridge University Press, Cambridge, UK.
- Yates D. E., Levine S., and Healy T. W. (1974) Site-binding model of the electrical double layer at the oxide/water interface. *J. Chem. Soc., Faraday. Trans.* **70**, 1807–1818.
- Zalac S. and Kallay N. (1992) Application of mass titration to the point of zero charge determination. *J. Colloid Interface Sci.* **149**, 233–240.
- Zeltner W. A. and Anderson M. A. (1988) Surface charge development at the goethite/aqueous solution interface: Effects of CO₂ adsorption. *Langmuir* **4**, 469–474.